Available online at www.sciencedirect.com
ScienceDirect
Nuclear Science and Techniques 19 (2008) 236–240
NUCLEAR SCIENCE AND TECHNIQUES

Numerical simulation of high-energy neutron radiation effect of scintillation fiber

MA Qingli[1,*] TANG Shibiao[2] ZOU Jiwei[3]

[1] *Electronics Department, Electronic Engineering Institute, Hefei 230038, China*

[2] *Department of Modern Physics, University of Science and Technology of China, Hefei 230026, China*

[3] *Department of Scientific Research, Electronic Engineering Institute, Hefei 230038, China*

Abstract Due to their low cost, flexibility, and convenience for long distance data transfer, plastic scintillation fibers (PSF) have been increasingly used in building detectors or sensors for detecting various radiations and imaging. In this paper, GEANT4 Monte Carlo simulation tool was used to obtain some radiation effects of PSF under high-energy neutron irradiation. BCF-20, a plastic fiber material, produced by Saint-Gobain, was used in the simulation. The fiber consists of a core scintillating material of polystyrene and an acrylic outer cladding. Incident neutrons produce energy deposition in fiber through neutron induced recoil proton events. The relationships between energy deposition efficiency and fiber length, fiber radius and incident neutron energy are presented. The variation with those parameters and parameter selection are also analyzed.

Key words Radiation effect, High-energy neutron, Scintillation fiber

CLC number TL91

1 Introduction

X-ray radiography and thermal neutron radiography have been used successfully in non-destructive examination (NDE) of various materials. However, the techniques are severely handicapped by their limitation to relatively thin objects. Fast neutron radiography can inspect much thicker objects, including composites, ceramics, or rubber[1]. In particular, it is ideal for objects composed of hydrogen-rich materials, where it is difficult to acquire high-quality images with thermal neutron and X-ray radiography[2].

As X-rays, electromagnetic radiations of short wavelengths, interact with orbit electrons of an atom, the cross section of the interaction increases with the atomic number of the atom. Neutrons are not the case. They interact with the neutrons and protons of a nucleus. Generally, neutrons penetrate materials easily, but some materials are exceptions to this rule and can be imaged readily. At present, few neutron imaging detectors provide high quantum efficiency for fast neutrons. Most existing detectors were developed for neutron radiography with collimated thermal neutron beams[3], such as, scintillator +CCD-camera, imaging plates, amorphous silicon flat panel, and CMOS pixel detector[4]. The first is the most popular detector for fast neutron radiography[5-7]. An interesting development is the scintillating fiber[8-12], which possesses high efficiency of fast neutron capture, good position resolution, lowcost, and the possibility of large-area detectors.

In order to learn general characteristics of the scintillation fiber, the relationships between energy deposition efficiency and fiber length, fiber radius and incident neutron energy were studied through GEANT4 simulation in this article. Variations of the parameters and parameter selection are analyzed. The results may be useful for the parameter selection in practice.

Supported by National Natural Science Foundation (No.60602065)
* Corresponding author. *E-mail address:* qinglima@gmail.com
Received date: 2008-04-25

2 Scintillation fibers

In recent years, the plastic scintillation fiber (PSF) has been applied in many fields, such as neutron imaging, particle discrimination, calorimeters, etc[13-17]. The main advantages of PSF are its fast response, flexibility and electromagnetic immunity[18].

Most common available scintillation fibers are made of either polymers or silica glasses. The materials are usually doped with cerium or terbium to improve their photoelectric absorption[19]. For neutron detection, we do not expect that the two kinds of materials would differ significantly. Therefore, BCF-20, a common plastic scintillation fiber, was chosen for our simulation. The results should be applicable to other types of PSFs. The core of BCF-20 fiber is made of polystyrene (PS) doped with 1% butyl-phenyl-byphenylyloxadiazole (PBD). The refractive index and density of the fiber are 1.60 and 1.05 $g \cdot cm^{-3}$, respectively. Pure PS has an emission spectrum in 300~350 nm, which is not suitable to common photodetectors. It is therefore necessary to dope PS with about 1% of some primary fluor to reach a scintillation efficiency of about half of that of crystalline anthracene and with about 0.01% of secondary fluor to shift the light emitted by the primary fluor to the region of maximum sensitivity of the absorption region of the photo-detector[18]. The cladding material of BCF-20 fiber is PMMA (polymethylmethacrylate) and has refractive index of 1.49. The thickness of the cladding layer is about 3% of core diameter. The calculated numerical aperture of the fiber is 0.58, the trapping efficiency is 3.44%, the number of emission light per MeV is about 8000 photons, the emission spectrum is peaked at 492 nm, and the decay time is 2.7 ns, according to the manufacturer[19]. The fiber structure is shown in Fig.1.

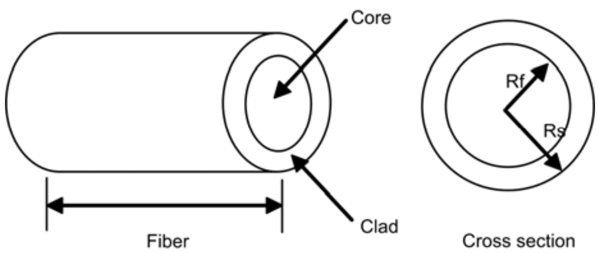

Fig.1 Structure of the fiber.

3 Computer simulation

The simulation was carried out using a Monte-Carlo code, GEANT4[20,21], which is a toolkit package developed at the European Organization for Nuclear Research (CERN) for simulating the performance of detectors used in nuclear and high energy physics. It has been used in many other applications, such as fluid dynamics and medical physics. It traces the trajectories of particles and their interactions with the materials. The results obtained with GEANT4 are consistent with those obtained using other programs[22-25].

The main data driven models in GEANT4 deal with neutron and proton induced isotope production, and with the detailed transport of neutrons at low energies (up to 20 MeV). The interactions of neutrons in the energy range are divided into four parts analogous to the other hadronic processes in GEANT4. We considered radiation capture, elastic scattering, fission and inelastic scattering as separate models[26]. These models comply with the interface for use with the GEANT4 hadronic processes which enable their transparent use within the GEANT4 tool-kit together with all other GEANT4 compliant hadronic shower models. All cross-section data are taken from the ENDF/B-VI[27] evaluated data library. A low energy limit for particle interaction is defined corresponding to the minimal energy within the validity range of the model[20]. Users can alternatively define a higher threshold for any specific application.

It is important for us to know the fiber's radiation effect of fast neutrons. The geometrical structure of detector in the simulation is given in Fig.2, with a plane neutron source placed across the center of the fiber, 10 cm away, which is not present in the figure. The neutron source has the same area as the cross section of the fiber. The simulation covers a relative broad energy range for the incoming neutrons, from 10 keV to about 10 MeV.

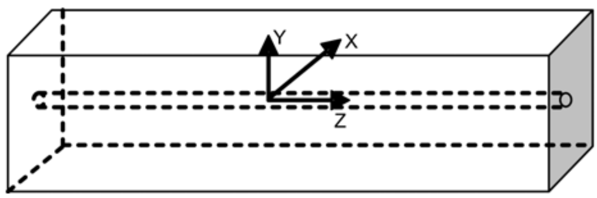

Fig.2 Geometrical structure of the detector.

4 Simulation results

4.1 Good-event rate

As an important parameter of a neutron imaging detector, good-event rate (GER) is defined as the probability for an incident photon to generate a good event in the fiber, i.e. the ratio of interacted photon number to total number of incident photons. The simulated GER versus fiber length and neutron energy are plotted in Fig.3 and Fig.4. As can be seen, except for 14 MeV neutrons, the GER varies little with fibers in lengths of more than 10 cm. And little change in GER is seen with neutrons of <1 MeV. However, it falls rapidly when the energy exceeds 1 MeV. This is of help for selecting appropriate neutron energy to achieve greater efficiency.

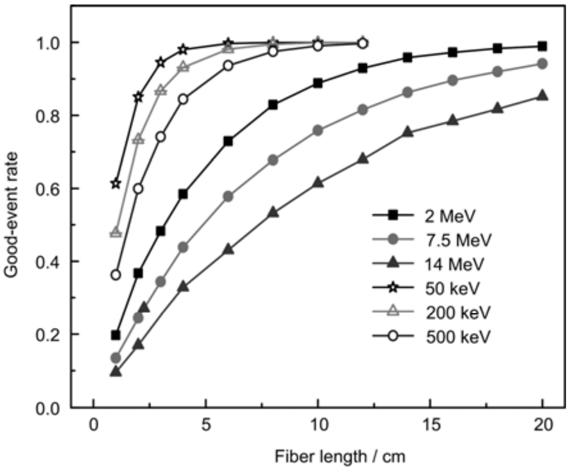

Fig.3 The good-event rate *vs*. fiber length for neutrons of different energies.

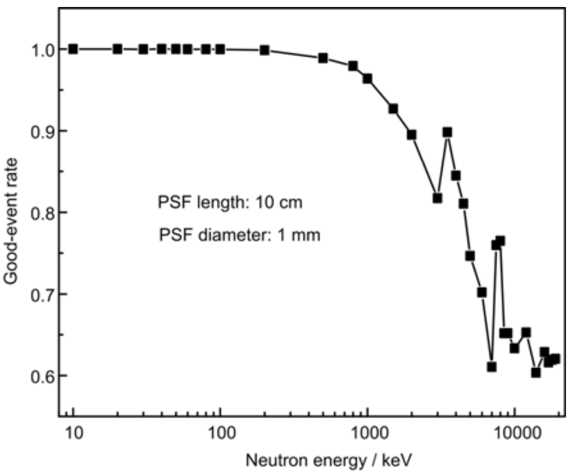

Fig.4 The good-event rate of neutrons at different energies.

4.2 Relationship between energy deposition efficiency and fiber length

The energy deposition of neutrons in a fiber can be characterized by an energy deposition efficiency (EDE), which is defined as the ratio of the energy deposited in the fiber to the incident neutron energy[28,29]. The simulated results are given in Fig.5. In Fig.5a, for low-energy neutrons (≤500 keV), the deposition efficiency reaches saturation at the fiber length of about 6 cm. For higher energy neutrons (2~14 MeV) in Fig.5b, where the energy deposition efficiency is lower than the low energy neutrons, the EDE increases slowly with the fiber length. For 14 MeV neutrons, the efficiency is about 12% with a fiber of 10 cm in length, and 17.5% with a 20 cm fiber. In view of the above results, a 10 cm fiber was chosen for the following simulations.

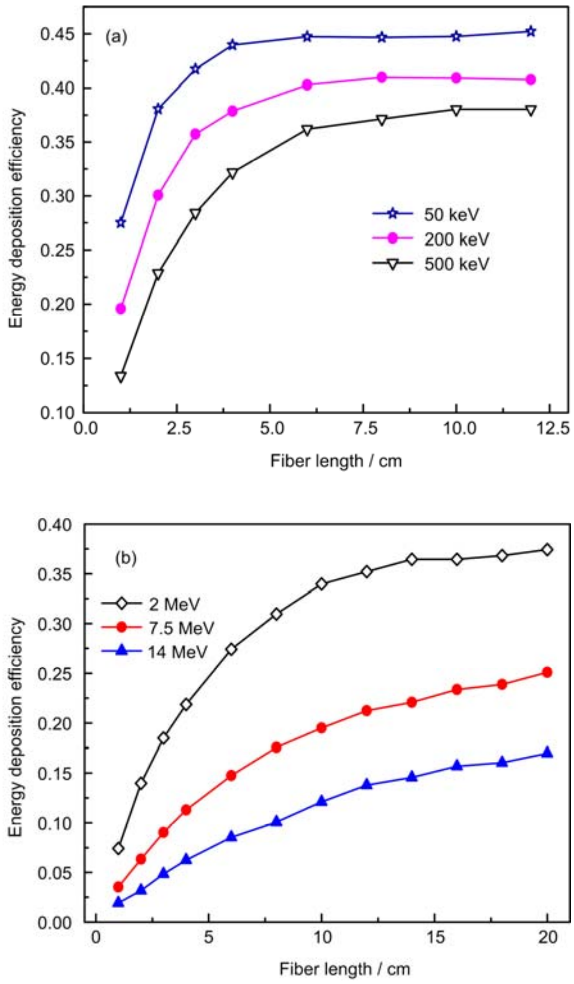

Fig.5 Energy deposition efficiency *vs.* fiber length for neutrons of different energies.

4.3 Relationship between EDE and fiber radius

Fiber radius is an important parameter for good image quality. It cannot be too small (causing too low EDE, or poor image contrast), nor too big (with increased pixel size, or decreased spatial resolution). On the other hand, the mechanism that causes the saturation described above could be the leakage of the secondary particles produced by incident neutrons. Therefore, we simulated the EDE for neutrons of given energies in a single fiber of different diameters. Some of the results are plotted in Fig.6. As can be seen, for low-energy neutrons (50 keV to 2 MeV), the EDE is high enough to achieve good image contrast, however, the EDE is low for high-energy neutrons (higher than 7.5 MeV), which is only less than 0.25. Therefore, there should be severe cross-talk effects for those high-energy neutrons. On the other hand, for the neutrons higher than 7 MeV, the EDE increases slowly with the radius from 0.5 mm to 50 mm. With 7.5 MeV incident neutrons, the efficiency is about 0.2, 0.23, 0.32, for radius of 0.5 mm, 10 mm, and 50 mm, respectively, that is, 19 mm increased pixel (2 double 9.5 mm) corresponding to only 0.03 improvement of EDE, which is not deserved. As a result, to balance the EDE and pixel size, we select a 0.5 mm radius in the following simulation.

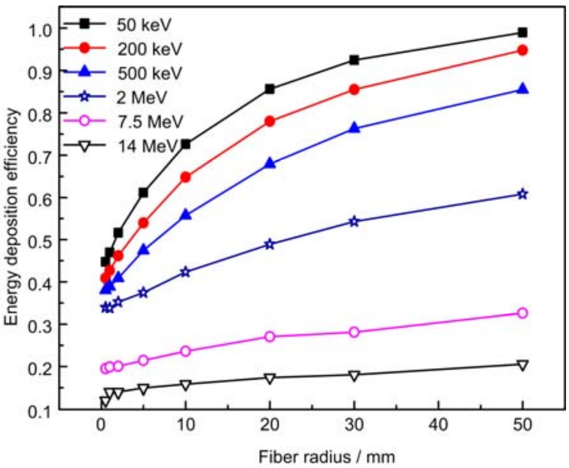

Fig.6 Energy deposition efficiency *vs.* fiber radius for neutrons of different energies.

4.4 Relationship between EDE and incident neutron energy

The EDE in PSF differs greatly for incident neutrons of different energies. In practice, the neutron energy can be adjusted to achieve an excellent efficiency. The EDEs for 10 keV~20 MeV neutrons bombarding a fiber of Φ1mm×10cm are given in Fig.7. The EDE decreases slowly with energy for neutrons of 1~3 MeV, and faster for neutrons of >3 MeV. In practice, we should choose appropriate neutron energy in this regard.

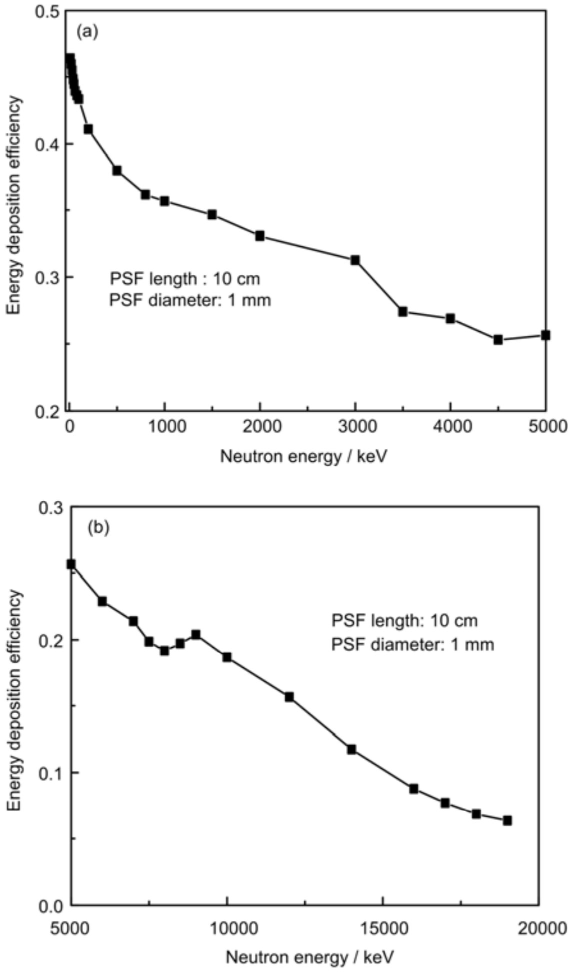

Fig.7 Energy deposition efficiency of neutrons of < 5MeV (a) and ≥5 MeV (b).

5 Conclusions

As an excellent non-destructive evaluation method, fast neutron radiography attracts more and more interests in the world. Due to its low cost, flexibility, and convenience for long distance data transfer, especially big reaction cross-section with neutrons, PSF has been widely used in building detectors or sensors for detecting neutrons. Radiation effects of PSF under high-energy neutron irradiation are obtained through GEANT4 simulation tool. It was found that the good-event rate varies little when the fiber length is more than 10 cm, hence an appropriate fiber length of 10 cm, and the energy deposition efficiency increases with the fiber radius and length. The present results are of theoretic significance in selecting reasonable fiber length and incident neutron energy for future experiments.

References

1 Kim K H, Klann R T, Raju B B, Nucl Instr Meth Phys Res A, 1999, **422:** 929-932.

2 Lehmann E H. Lecture Notes in Physics, 2006, **694:** 231-249.

3 Cluzeau S, Huet J, Letourneur P. Nucl Instr Meth Phys Res B, 1994, **89:** 432-436.

4 Lehmann E H, Vontobel P, Frei G, *et al*. Nucl Instr Meth Phys Res A, 2004, **531:** 228-237.

5 Mikerov V, Waschkowski W. Nucl Instr Meth Phys Res A, 1999, **424:** 48-52.

6 Mikerov V I, Zhitnik I A, Barmakov J N, *et al*. Appl Radiat Isotop, 2004, **61:** 529-535.

7 Lehmann E, Frei G, Nordlund A, *et al*. IEEE Trans Nucl Sci, 2005, **52:** 389-393.

8 Ress D, Lerche R A, Ellis R J, *et al*. Proceedings of SPIE – The International Society for Optical Engineering, 1994, **2281:** 95-112.

9 Zhang Q, Wang Q, Xie Z, *et al*. Nucl Instr Meth Phys Res A, 2002, **486:** 708-715.

10 Ress D, Lerche R A, Ellis R J, *et al*. Rev Sci Instr, 1995, **66:** 4943-4948.

11 Fujine S, Yoneda K, Yoshii K, *et al*. Nucl Instr Meth Phys Res A, 1999, **424:** 190-199.

12 Nasseri M M, Yin Z, Wu X, *et al*. Nucl Instrum Methods Phys Res B, 2004, **225:** 617-622.

13 Tang S B, Ma Q L, Yin Z J, *et al*. Appl Radiat Isotop, 2008, **66:** 162-167.

14 Tang S, Ma Q, Fang J, *et al*. IEEE Trans Nucl Sci, 2007, **54:** 1773-1778.

15 Tang S B, Yin Z J, Ma Q L, *et al*. Nucl Instrum Methods Phys Res A, 2003, **506:** 250-303 B, 2007, **263:** 441-445.

16 Mengesha W, Mascarenhas N, Peel J, *et al*. IEEE Nuclear Science Symposium Conference Record – Nuclear Science Symposium and Medical Imaging Conference, 2005, 535-539.

17 Mengesha W, Mascarenhas N, Peel J, *et al*. Proceedings of SPIE – The International Society for Optical Engineering, 2005, **5923:** 1-8.

18 White T O. Nucl Instrum Methods Phys Res A, 2003, **506:** 250-303 A, 1988, **273:** 820-825.

19 Bicron Corporation web site, 2003. http://www.bicron.com.

20 Agostinelli S, Allison J, Amako K, *et al*. Nucl Instrum Methods Phys Res A, 2003, **506:** 250-303.

21 Allison J, Amako K, Apostolakis J, *et al*. IEEE Trans Nucl Sci, 2006, **53:** 270-278.

22 Carrier J F, Archambault L, Beaulieu L. Med Phys, 2004, **31:** 484-492.

23 Aso T, Kimura A, Tanaka S, *et al*. IEEE Trans Nucl Sci, 2005, **52:** 896-901.

24 Amako K, Guatelli S, Ivanchencko V, *et al*. Nucl Phys B-Proc Suppl, 2006, **150:** 44-49.

25 Amako K, Guatelli S, Ivanchencko V N, *et al*. IEEE Trans Nucl Sci, 2005, **52:** 910-918.

26 GEANT4 Physics Reference Manual. http://geant4.web.cern.ch/geant4.

27 Tuli J. Evaluated Nuclear Structure Data File, BNL-NCS-51655-Rev87, 1987.

28 Knoll G F. Radiation detection and measurement. New York: John Wiley & Sons, 1979.

29 Leroy C. Principle of radiation interaction in matter and detection. Singapore: World Scientific Publication, 2004.